ELSEVIER

Journal of Nuclear Materials 241–243 (1997) 294–298

journal of nuclear materials

Assessment of erosion and surface tritium inventory issues for the ITER divertor [1]

J.N. Brooks [a,*], R. Causey [b], G. Federici [c], D.N. Ruzic [d]

[a] *Argonne National Laboratory, 9700 S. Cass Avenue, Argonne, IL 60439, USA*
[b] *Sandia National Laboratories, P.O. Box 969, Livermore, CA 94550, USA*
[c] *ITER JWS Garching Co-center, Boltzmannstrasse 2, 85748 Garching, Germany*
[d] *University of Illinois, 103 S. Goodwin Avenue, Urbana, IL 61801, USA*

Abstract

We analyzed sputtering erosion and tritium codeposition for the ITER vertical target divertor design using erosion and plasma codes (WBC/REDEP/DEGAS +) coupled to available materials data. Computations were made for a beryllium, carbon, and tungsten coated divertor plate, and for three edge plasma regimes. New data on tritium codeposition in beryllium was obtained with the tritium plasma experiment (TPE) facility. This shows codeposited H/Be ratios of the order of 10% for surface temperatures ≤ 300°C, beryllium thereby being similar to carbon in this respect. Hydrocarbon transport calculations show significant loss (10–20%) of chemically sputtered carbon for detached conditions ($T_e \approx 1$ eV at the divertor), compared to essentially no loss (100% redeposition) for higher temperature plasmas. Calculations also show a high, non-thermal, D–T molecular flux for detached conditions. Tritium codeposition rates for carbon are very high for detached conditions ($\sim$ 20 g T/1000 s discharge), due to buildup of chemically sputtered carbon on relatively cold surfaces of the divertor cassette. Codeposition is lower ($\sim$ 10X) for higher edge temperatures ($\sim$ 8–30 eV) and is primarily due to divertor plate buildup of physically sputtered carbon. Peak net erosion rates for carbon are of the order of 30 cm/burn yr. Erosion and codeposition rates for beryllium are much lower than for carbon at detached conditions, but are similar to carbon for the higher temperatures. Both erosion and tritium codeposition are essentially nil for tungsten for the regimes studied.

Keywords: ITER; Erosion and particle deposition; Tritium inventory; Low Z wall material; High Z wall material

1. Introduction

A recent paper [1] summarized initial work on surface related tritium issues for ITER. This paper extends the analysis, specifically for the divertor. In particular, the effect of different materials and edge plasma regimes, and the transport of chemically sputtered hydrocarbons for detached conditions has been examined. We have also obtained critically needed data for H/Be codeposition at elevated temperatures. This work is also, in part, a follow up to Ref. [2] which analyzed erosion for a gas-bag type ITER configuration. Since the plasma solutions available to date are still evolving, are partially inconsistent in assumptions with each other, and are speculative to various degrees, the intent of this analysis is on defining broad trends. More research will be needed to develop reliable design information for ITER, or any fusion tokamak.

2. Hydrogen/beryllium codeposition experiment at TPE

2.1. Procedure

The TPE facility [3] was used for measurements of the amount of tritium retained in a sputter deposited beryllium film produced by the sputtering of beryllium with a hydro-

* Corresponding author. Tel.: 630 252 4830; fax: 630 252 5287.
[1] U.S. work was supported by the U.S. Department of Energy.

PII S0022-3115(96)00517-X

gen isotope plasma. A 2.54 cm radius beryllium disk was used as the sputter source. The 0.3 cm radius aluminum or copper catcher plate for the sputtered beryllium was located approximately 5 cm from the plane of the beryllium disk and 5 cm from the disk centerline. The miniature catcher plate was heated by a Varian™ heater. A small aluminum sleeve with an attached thermocouple was placed around the plate to hold it in place. The plasma used to generate the sputtered beryllium, as determined by calibrated flow meters, consisted of 90% deuterium and 10% tritium. Base pressure in the system was approximately 1×10^{-5} Pa and consisted primarily of water vapor. The beryllium sample was biased to give the D and T ions an energy of 100 eV.

An experiment began with the heating of the catcher plate to the desired operating temperature before the ignition of the plasma. The plasma was started using pure deuterium. The beryllium disk was then biased and the plasma intensity increased until the deuterium flux ($\sim 80\%$ D_1^+, $\sim 20\%$ $D_2^+ + D_3^+$) on the beryllium sample was 1.1 A (3.3×10^{21} D/m^2 s). At this time, tritium was added to the plasma gas, and the one hour codeposition period 'officially' began.

At the end of one hour, the source was turned off, and the sputter-coated sample was allowed to cool. This sample was then placed in a small furnace where the temperature was ramped linearly up to 1073 K. During the heating, gas consisting of 99% helium and 1% protium was swept over the sample. This gas with the collected tritium was sent first through an ionization chamber. Upon exiting the ionization chamber, 10% oxygen was added to the gas. The mixture was then sent over a copper oxide bed heated to approximately 823 K. The hydrogen isotopes were converted to water by this process and collected by glycol bubblers next in line. The amount of tritium released from the catcher plate was determined both by the calibrated ionization chamber and by scintillation counting of the glycol–water solution. The amount of tritium collected was multiplied by 10 to give the total amount of hydrogen isotopes retained in the sputtered beryllium film.

2.2. Results

Elastic recoil detection analysis (ERDA) was used to measure the amount of beryllium in the film collected on a copper catcher plate at 373 K (one sample was prepared with deuterium alone). Approximately 6×10^{16} Be/cm^2 was measured. The measurement at 573 K was performed using an aluminum catcher plate after it was noticed that an earlier experiment at that temperature with copper suggested interdiffusion of the beryllium and the copper. Two experiments were performed at 473 K, one with an aluminum catcher plate and one with a copper plate. The ratio of hydrogen isotope to beryllium in the samples was: 0.35 for 373 K; 0.18 and 0.14 for 473 K; and 0.03 for 573 K. While the retention in the copper catcher plate at 473 K was slightly greater than that for the aluminum plate, the difference was not considered significant.

The results presented here agree with the findings of Mayer et al. [4] where a 4.5 keV D_3^+ beam was used to sputter beryllium onto a silicon catcher plate. In those experiments, a ratio of D/Be of 0.38 was measured at room temperature. Mayer et al. reported carbon to also exist in their layer at a level somewhat below that of the deuterium. In the present experiments, carbon was seen during the analysis, but only at trace levels. It can be concluded that carbon is not a controlling factor in these measurements. The results also agree with those of Wampler [5] where beryllium samples were saturated with 0.5 and 1.5 keV deuterons. The retention at saturation was 0.31 D/Be. Wampler's samples were annealed after saturation at 50 K intervals for 10 min at each interval. The retention versus temperature for his results agree very well with the values determined in this report for saturation at temperature.

3. Computational model for erosion and codeposition

We modeled the ITER vertical target divertor design [6]. This design has a solid divertor plate that receives most of the ion and heat flux, a louvered region opposite the plate surmounted by the dome which defines the private region, and several other surfaces e.g., cassette body liners. We focus on the outer divertor region and scale tritium results for the whole system, i.e. inner and outer divertors. We use as input a basic set of 2-dimensional D–T plasma parameters for the divertor region. The D–T ion flux to the plate is given by $\Gamma_i = N_i C_s \sin(\theta)$, for sound speed C_s, ion density N_i, and magnetic field-to-surface angle $\theta = 1.5°$. The DEGAS + code [7] is then used to compute atomic and molecular D–T flux to the divertor, for the detached regime, but not at present for the other regimes. The WBC [8] and REDEP [9,10] codes are then used to compute sputtering and the resultant impurity transport. The dual-region (magnetic and Debye) sheath model of Ref. [8] is used in all cases. Transport back to the plate, if any, is followed in detail, but transport to the other surfaces is computed in a simplified manner for this study.

Parameters for a detached plasma solution were taken from the (preliminary) work of Kukushkin [11]. This shows plasma temperatures of $T_e \approx T_i \approx 1$–$1.5$ eV, and electron densities of $N_e \approx 10^{19}$–10^{21} m^{-3} along the divertor plate. 'Radiative' regime parameters are taken from the work of Schneider et al. [12] for a $\sim 1\%$ neon/D–T plasma. This shows a substantial reduction of convected heat load to the plate compared to a high recycle solution, fairly low plasma temperatures, but not full detachment. Finally, a 'high-recycle' plasma was defined using the parametric model of [10], with a peak heat load of 8 MW/m^2 (probably lower than obtainable), peak sheath temperature of $T_e = T_i = 30$ eV, and temperature and density e-folding

parameters $\delta_t = 0.03$ m, $\delta_n = 0.04$ m. It should be noted that these solutions are inconsistent, differing in important respects such as input power to the scrape off layer, midplane density, and treatment of neutrals.

The plate surface temperature is computed as a function of material coating and heat flux, for the ITER water-cooled design. Hydrogen trapping fractions for carbon are given by the surface temperature dependent model of Ref. [13]. H/Be fractions are given by the above TPE results scaled linearly for 100–300°C and scaled two ways for > 300°C (1: same as 300°C value, i.e. 3% H/Be, and 2: linearly reduced with the same slope as from 100–300°C).

Ref. [14] gives details of chemically sputtered hydrocarbon transport models used in the WBC code. A key update is the inclusion of elastic collisions between hydrocarbons and D–T ions and neutrals. Briefly, thermal methane is launched. Carbon/hydrocarbon particles collide with the plasma through elastic and inelastic collisions, and undergo Lorentz force motion. The 34 atomic and molecular reactions of Ref. [15] are followed. Redeposited particles stick or are reemitted according to the species-dependent model of Ref. [14], such model tending to be confirmed by recent data [16].

4. Results

4.1. Carbon coating-detached regime

The most striking result of the DEGAS + solution is a high D–T molecular flux, of order 10X the ion flux, and with energies in the 3 to 5 eV range. These are due to surface emitted thermal molecules that charge exchange with the faster flowing D–T ions producing a fast flowing molecule that scatters off the field line and strikes the surface. This does not happen at higher plasma temperatures because the molecules are rapidly dissociated by electrons and so do not remain intact. In contrast to the molecules, the predicted ratio of atom to ion flux, i.e. ~ 0.5, is similar to other regimes. It should be noted that the effect of the high molecular flux on the ion parameters, if any, has not been self-consistently computed.

Carbon erosion in this regime occurs due to the so-called 'room temperature' type chemical sputtering, with essentially no physical sputtering. Hydrogen ion impingement energies are of the order of 5–10 eV (depending on the precise T_e, sheath potential, and flow velocity). Hydrogen atom energies are of order 5 eV. There is no chemical sputtering coefficient data for these low energies. Chemical sputtering mechanisms have been recently assessed by Roth and Garcia-Rosales [17]. Based on the theory of [17] we have used a computational value of $Y_{chem} = 0.01$ for the D–T ions and atoms. This is much lower that the value of ~ 0.05 observed at higher energies, e.g. Ref. [17,18], but is based on consideration of possible threshold effects. Non-thermal molecular sputtering coefficients are highly uncertain. We have used a range of values for this study with an assumed 'reference' value of $Y_{H_2-C} = 0.001$.

The WBC results show that about 10 to 20%, depending on plate location, of chemically sputtered particles are not locally redeposited, i.e. on the divertor plate, but instead travel completely across the divertor region to the plenum and other surfaces. A typical reaction sequence for escaping particles is as follows: $CH_4 \rightarrow CH_4^+ \rightarrow CH_3 \rightarrow CH_3^+ \rightarrow CH_2 \rightarrow CH_2^+ \rightarrow CH \rightarrow CH^+ \rightarrow C$. The carbon atom so formed generally undergoes no further reaction due to the low plasma temperatures in most of the divertor region. (At these low temperatures the reactions occurring are primarily electron recombination and proton ionization, but not electron ionization.) The carbon atom then redeposits or escapes, depending on it's velocity at formation and on subsequent elastic collisions.

The net erosion profile for carbon is shown in Fig. 1. (An 80 cm wide segment along the target is shown, with the distance parameter going from top to bottom.) Table 1 summarizes results for this and other cases. Due to the high loss fractions net erosion is always positive along the divertor vertical plate — growth of carbon occurs on other surfaces. The gross erosion rate is about 10 times higher than the net — this raises concerns about the properties (thermal, mechanical, etc.) of the redeposited material. The tritium codeposition rate was computed based on the computed carbon growth rate and a surface temperature of 150°C for the 'cold' surfaces. The resulting codeposition of 21 g T for a 1000 s ITER pulse is very high. Both erosion and tritium codeposition vary substantially with the molecular chemical sputtering coefficient.

4.2. Beryllium coating-detached regime

A key finding for this regime is that any beryllium atoms that are sputtered do not locally redeposit — due to the very low rate coefficient for electron impact ionization. This contrasts with the 90–100% redeposition rate typical of higher temperature regimes. The critical issue is whether there is any sputtering. Low energy data is lacking. Both hydrogen and helium impingement energies are below

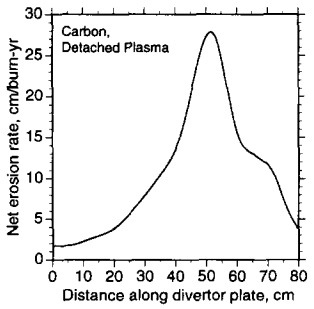

Fig. 1. Net erosion profile for carbon divertor surface, detached plasma regime.

Table 1
Summary of ITER divertor erosion and tritium codeposition analysis

Plasma regime (peak T_e at divertor)	Divertor coating	Peak gross erosion rate (cm/burn yr)	Peak net erosion rate (cm/burn yr)	Tritium co-deposition rate [a] (g T/1000 s discharge)	Primary location of codeposition
Detached (~ 1.5 eV)	carbon	242 (161–963) [b]	27 (14–119) [b]	21 (12–106) [b]	non-plate [c]
	beryllium	(0–1) [d]	(0–1) [d]	(0–0.4) [d]	non-plate
Radiative (~ 8 eV)	carbon	758	18	1.3	plate
	beryllium	689	32	(2.0–4.0) [e]	non-plate
	tungsten	0.5	< 0.01	~ 0	—
High-recycle (~ 30 eV)	carbon	1090	46	2.6	plate
	beryllium	1500	59	3.0	non-plate
	tungsten	5	< 0.1	~ 0	—

[a] Total for inner and outer divertor system (does not include any tritium trapping due to first wall, limiter, etc. erosion).
[b] Range of values computed for possible variations in D–T molecule chemical sputtering coefficient, range shown is for $Y_{H_2-C} = 0$–0.01.
[c] Plenum region, dump plate, etc.
[d] Highly uncertain due to lack of data on He–Be low energy, oblique incidence, sputtering coefficient; range shown is for $Y_{He-Be} = 0$–0.001.
[e] Uncertain due to lack of data on all sputtering coefficients at low energy, and trapping with surface temperature for above 300°C; range shown is for span of calculations.

commonly computed sputtering thresholds, but this concept is based on binary collision theory. Molecular-dynamic considerations give rise to the possibility of non-zero sputtering for impinging particle energies above the surface binding energy. A particular issue is sputtering by the ~ 10% content helium ions. Trace impurities such as oxygen (order of 0.1%) and radiating impurities (e.g. neon) may also sputter. The impinging helium energy depends on the charge state (via sheath acceleration), plasma flow entrainment, and exact plasma temperature. These are not well specified at present by the plasma solutions. A rough estimate leads to a plausible helium impingement energy range of 5–15 eV, with incidence at ~ 60° from the normal. The binary-collision VFTRIM code [19] was used to calculate the He–Be sputtering yield for these conditions. The yield range is 0 to 9×10^{-4}. Using this, possibly lower bound, yield range gives the erosion and tritium rates shown in Table 1. Both rates are much lower than for carbon but tritium codeposition may still be significant.

4.3. Higher temperature regimes

Figs. 2 and 3 show the net erosion profiles for carbon and beryllium for the radiative regime. Their behavior is qualitatively similar and shows a complex pattern of erosion/growth on the plate. The oscillatory nature is due to small variations in the plasma parameters at the plate, for the solution employed. The gross erosion profiles (not shown) are much smoother, net erosion being a fine balance between high sputtering and redeposition fluxes. Most net carbon erosion is due to physical and not chemical sputtering in this regime, although the latter is still important at lower plasma temperature areas along the divertor plate. An important point for both materials is that net growth tends to occur on colder surface (lower heat flux) regions of the plate, as well as the colder non-plate regions. There is a general transfer of material from top to bottom along the plate — as follows from the ~ 15° angle of the poloidal field. Because of the selective trapping on colder areas the tritium retention tends to be insensitive to peak heat loads which mostly affect the near-strike point region. Results for tungsten show small gross erosion due only to a trace (~ 0.1%) oxygen content, and very low net erosion due to nearly 100% local redeposition.

As summarized in Table 1, the results for the high recycling regime are qualitatively similar to the radiative regime, for the low Z materials. The key difference from previous analysis, e.g. Ref. [8], is the prediction of signifi-

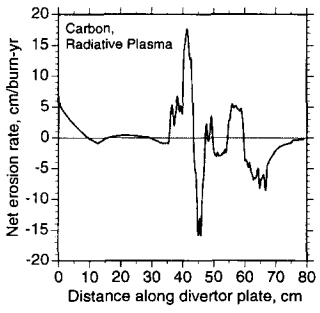

Fig. 2. Net erosion profile for carbon divertor surface, radiative plasma regime.

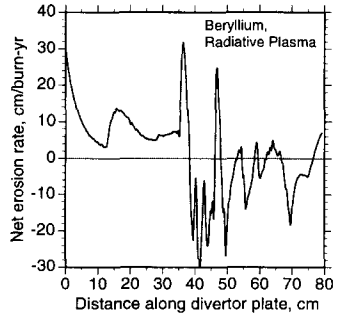

Fig. 3. Net erosion profile for beryllium divertor surface, radiative plasma regime.

cant tritium codeposition for beryllium. This follows from using the new TPE data instead of the previous assumption of low tritium codeposition at elevated surface temperatures. Tungsten erosion increases in this regime but is still very low. Tritium codeposition for tungsten is zero, within computational error, due to very little growth, and such growth only occurring near the higher surface temperature ($\sim$ 1000°C) strike point region of the divertor plate where the codeposition ratio is essentially zero.

5. Discussion

Implications for the performance and safety of the ITER device resulting from the tritium codeposition inventory and plate erosion lifetime for most of the C and Be cases, are large and would need counteracting measures. In particular, we would need reliable and efficient cleaning methods that would periodically remove tritium from the codeposited layers (either adhering onto the plasma facing component surfaces or in the form of flakes possibly collecting on the bottom of the divertor cassette). Helium–oxygen glow discharge cleaning has been used with some success to remove surface tritium in existing machines. However, the rather low cleaning efficiency anticipated for ITER conditions and the resulting oxygen contamination of the plasma facing surfaces raises concerns for subsequent plasma operation. Alternative cleaning techniques and various other solutions need investigation.

6. Conclusions

This work has identified several trends which can help guide material selection and operating regimes for a fusion reactor. For a carbon divertor plate coating, the use a low but not detached plasma edge regime can minimize sputtering erosion and tritium codeposition. Use of carbon in a detached regime would appear to raise serious concerns about surface tritium inventories. Beryllium is much better than carbon at detached conditions but not for other regimes. Tungsten is far superior, in the respects analyzed. Considerable uncertainties apply to many of these findings. Major uncertainties include the effect of oxygen on beryllium codeposition properties, low energy physical and chemical sputtering coefficients, and the transport of helium ions and hydrogen molecules for detached conditions. Data and analysis is needed in these areas as well as analysis of erosion and tritium codeposition from other plasma facing components.

Acknowledgements

We would like to thank R. Turkot, Jr. (UIUC) for performing He–Be VFTRIM calculations.

References

[1] G. Federici et al., Proc. of the 16th IEEE/NPSS Symp. on Fusion Engineering, IEEE #95CH35852 (1995) 418.
[2] J.N. Brooks, D.N. Ruzic, D.B. Hayden and R.B. Turkot, Jr., J. Nucl. Mater. 220–222 (1995) 269.
[3] R.A. Causey, D. Buchenauer, W. Harbin, D. Taylor and R. Anderl, Fusion Technol. 28(3) (1995) 1144.
[4] M. Mayer, R. Behrisch, H. Plank, J. Roth, G. Dollinger and C.M. Frey, J. Nucl. Mater., to be published.
[5] W.R. Wampler, J. Nucl. Mater. 122–123 (1984) 1598.
[6] K.J. Dietz et al., Fusion Eng. Des. 27 (1995) 96.
[7] D.N. Ruzic, Phys. Fluids B 5 (1993) 3140.
[8] J.N. Brooks, Phys. Fluids 8 (1990) 1858.
[9] J.N. Brooks, Nucl. Technol. Fusion 4 (1983) 33.
[10] J.N. Brooks, Fusion Technol. 18 (1990) 239.
[11] A. Kukushkin, personal communication (1996).
[12] R. Schneider et al., ISPP, Theory of Fusion Plasmas, eds. E. Sindoni et al. (SIF, Bologna, 1994) p. 273; D. Coster, personal communication (1995).
[13] J.N. Brooks, H.F. Dylla, A.E. Pontau and K.L. Wilson, Fusion Technol. 19 (1991) 1095.
[14] J.N. Brooks, ANL/FPP/TM-259, Argonne National Laboratory (1992).
[15] A.B. Ehrhardt and W.D. Langer, PPPL-2477 (1987).
[16] W. Wang, W. Eckstein, R. Schwörer, H. Plank and J. Roth, J. Nucl. Mater. 220–222 (1995) 1033.
[17] J. Roth and C. Garcia-Rosales, Analytic Description of the Chemical Erosion of Graphite by Hydrogen Ions, Nucl. Fusion, to be published.
[18] W. Poschenrieder et al., J. Nucl. Mater. 220–222 (1995) 36.
[19] D.N. Ruzic, Nucl. Instrum. Methods B 47 (1900) 118.